CALCULATION OF UNSTEADY LOADS FOR THE F/A-18 VERTICAL TAIL BUFFETING

M. Guillaume*, J. Vos, A. Gehri*, B. Bucher*, S. Merazzi***, Th. Ludwig***, G. Mandanis******

***RUAG Aerospace, **CFS Engineering, ***SMR SA, ****M@M GmbH**

Keywords: *Computational Fluid Dynamics, Loads, Fluid Structure Coupling, Aeroelasticity*

Abstract
For the Swiss F/A-18 Aircraft, the Boeing Company performed an Aircraft Structural Integrity Study (ASIP) to analyze the structural integrity of the entire airframe based on the Swiss design spectrum. To validate this study a full scale fatigue test were carried out at RUAG Aerospace. By setting up the test facility and preparing the fatigue test loads using data from the F/A-18 Original Equipment manufacturer (OEM) RUAG met some difficulties due to the sparse documentation. This situation pushed RUAG Aerospace to search for methods to generate independently aerodynamic loads for the F/A-18 and as a result a large investment was made in the development and implementation of Computational Fluid Dynamics (CFD). The Center Aerodynamics of RUAG Aerospace employs the Navier Stokes Multi Block (NSMB) computational fluid dynamics (CFD) code which was developed in an international collaboration. The CFD code was validated by comparing results of calculations with low speed wind tunnel results from RUAG Aerospace, and with loads data from the Boeing flight loads data base. For selected load cases unsteady calculations were made for a simulation time of 0.5 seconds. The fluctuating loads at the vertical tail due to the buffeting induced by the vortex of the leading edge extension went up to 2.5 times the averaged steady calculated value. Using the information of the CFD calculation a Swiss dynamic design spectrum was created and compared with the Boeing spectrum. First preliminary results for dynamic transient analysis on the F/A-18 vertical tail are presented here. The use of novel unsteady aero-elastic simulation should improve the design of modern aero structures due to buffeting and flutter problems in an early phase.

1. ABBREVIATIONS

ALE	Arbitrary Lagrange Eulerian
AOA	angle of attack
ASIP	Aircraft-Structural-Integrity-Program
BM	bending moment
CAD	Computer Aided Design
CFD	Computational Fluid Dynamic
CSM	Computational Structural Model
FEM	Finite Element Model
FSI	Fluid Structure Interaction
F_Z	force in global z direction
HT	horizontal tail
LEX	Leading Edge Extension
LBL	Line by line
MI	Modul Integration
NSMB	Navier Stokes Multi Block
MPI	Message Passing Interface
OEM	Original Equipment Manufacturer
PC	Personal Computer
Q	dynamic pressure
SH	shear force
SPMD	Single Program Multiple Data
TEF	Trailing Edge Flap
TQ	torque or torsion moment
W/O	without

2. INTRODUCTION

For the Swiss F/A-18 Aircraft, the Boeing Company performed an Aircraft Structural Integrity Study (ASIP) to analyze the structural integrity of the entire airframe based on the Swiss design spectrum (see figure 1). The Swiss maneuver spectrum was three times more severe than the US Navy design spectrum, but the dynamic spectrum was not more severe than the US Navy dynamic design spectrum. For the validation of the Swiss Redesign a full scale fatigue test was carried out at RUAG Aerospace. Only few relevant fatigue load cases for the entire airplane were obtained from The Boeing Company in St. Louis, the F/A-18 Original Equipment Manufacturer (OEM).
This situation pushed RUAG Aerospace to search for methods to generate independently aerodynamic loads for the F/A-18 and as a result a large investment was made in the development and implementation of steady and unsteady Computational Fluid Dynamics (CFD) calculations. To take the structural response of the structure into account a Fluid Structure Interaction (FSI) tool was developed. Furthermore an unsteady aero-elastic approach is in the final stage for the analysis of the F/A-18 vertical tail buffeting conditions. This effort provided RUAG Aerospace with the ability to predict component loads to be applied on the structure for steady

state and buffeting fatigue analysis. In addition, a tool was obtained which permitted to better understand the complicated flow field over the entire F/A-18 full flight envelope and to check some load cases delivered by the OEM.

3. COMPUTATIONAL FLUID DYNAMICS DEVELOPMENT WITH NSMB

3.1 The NSMB Solver

The calculations of the F/A-18 flow field were made using the NSMB Structured Multi Block Navier Stokes Solver. NSMB was developed from 1992 until 2003 in a consortium composed of four universities, namely EPFL (Lausanne), SERAM (Paris), IMFT (Toulouse) and KTH (Stockholm) and four industrial companies namely Airbus France, EADS (Les Mureaux), CFS Engineering (Lausanne) and SAAB Aerospace (Linköping). Since 2004 NSMB is developed in a new consortium lead by CFS Engineering and composed of RUAG Aerospace (Emmen), EPFL (Lausanne), EHTZ (Zürich), IMFT (Toulouse), IMFS (Strassbourg), the Technical University of München and the University of the Army in München.

NSMB employs the cell-centered Finite Volume method using multi block structured grids to discretize the Navier Stokes equations. Various space discretization schemes are available to approximate the inviscid fluxes, among them the 2nd and 4th order centered scheme with artificial dissipation, and 2nd, 3rd and 5th order upwind schemes. The viscous fluxes are approximated using a 2nd order approximation.
The space discretization leads to a system of ordinary differential equations, which can be integrated in time using either the explicit Runge Kutta scheme or the semi-implicit LU-SGS scheme. To accelerate the convergence to steady state the following methods are available:

- local time stepping
- implicit residual smoothing (only with the Runge Kutta scheme)
- full multi grid (grid sequencing)
- multi grid
- pre-conditioning for low Mach number
- artificial compressibility for incompressible flows

For unsteady flow calculations the 3rd order Runge Kutta scheme and the Dual Time Stepping method are available.

Different turbulence models have been thoroughly tested and validated for NSMB:

- Baldwin-Lomax algebraic model
- Spalart-Allmaras 1 equation model
- Chien k-ε 2 equations model
- Wilcox k-ω 2 equations model
- Menter Baseline and Shear stress k-ω 2 equations model

The ALE approach is available to simulate the flow on moving grids. Recently a re-meshing algorithm was implemented in NSMB to permit the simulation of the flows on deforming grids, as found for example in Fluid Structure Interaction problems.

NSMB has no limit on the number of blocks used in a calculation. Block interfaces do not need to be continuous since a sliding mesh block interface treatment is available.

The NSMB code was originally written in Fortran 77 and the code is at present a mix of Fortran 77 and Fortran 90. NSMB was parallelized using the master-slave paradigm in 1995, which was changed to the SPMD paradigm using MPI in 1998. NSMB is saved under cvs for revision control, and automatic testing scripts are used for testing each new release.

3.2 The F/A-18 Mesh

The most time consuming process in a CFD simulation is the generation of the grid. This involves different steps. First (if required) the CAD surface needs to be cleaned up, then a multi block topology needs to be set-up, and finally the mesh is generated. The latest mesh for the F/A-18 fighter was generated by Mindware in collaboration with the Center of Aerodynamics of RUAG Aerospace. This mesh has 2802 blocks and 13.9 million cells (see figures 2 and 3). The size of the mesh was increased at one hand due to the modelling of more details of the F/A-18 (antennas, LEX fence, …), at the other hand the surface mesh of the new mesh is much finer than on the old mesh. The volume mesh of the new mesh is almost doubled compared to the old mesh.

3.3 Aerodynamic Loads Extraction

To permit the calculation of the aerodynamic loads on different aircraft components it was decided to divide the aircraft in different components such as each component has a unique boundary condition type in NSMB. A post processing program was developed that computes the aerodynamic loads on each aircraft component, and translates it into American units.

3.4 Load Transfer Tool

At high angles of attack (which are typical for high g manoeuvres), the wing has to maintain a very high lift to carry the whole loads on the aircraft. As a result the wing deforms, which can be observed with the eye during the take off from the carrier or during the cycling of the full scale fatigue test. At the wing tip deformations of 0.3 m are quite frequent during a standard manoeuvre mission. One can expect that this change in wing shape will have an influence on the flow field over the wing, and thus on the aerodynamic loads. To investigate this effect a tool was developed to transfer the aerodynamic loads computed using CFD to the NASTRAN finite element model (FEM), and to transfer the computed displacements back to the CFD surface grid. Since the CFD surface grid and the mesh of the structural model are totally different (see figure 4) an interpolation procedure based on volume spline interpolation was implemented such as the computed aerodynamic forces are transferred to the set of structural nodes. NASTRAN then uses these forces to evaluate the corresponding deformation, which is then interpolated to the CFD mesh using again the volume spline interpolation. The re-meshing algorithm implemented in NSMB then generates a new CFD mesh. This method has proved its reliability not only for the smooth deflection of the overall wing but also for the deflection of the control surfaces, which are more sensitive.

4. STEADY STATE CFD CALCULATIONS

In all calculations discussed here it is assumed that the aircraft is perfectly symmetrical and only symmetrical load conditions were considered until now. Consequently only one half of the aircraft was used in the calculations.

4.1 Comparison of CFD Component Loads

The component loads of the F4 US Navy flight data base are very reliable measurements and were used to validate the CFD calculation. 15 load cases were simulated with the original mesh, taking into account the real flap positions. Also 12 Swiss load cases from the ASIP study were calculated for comparison.

The results (see figures 5 and 6) matched for all component loads very well with the exception of the vertical tail and the horizontal tail. If only loads with an AOA below 10° were considered the match was much better but still not fully satisfactory for the component loads of the vertical tail and the horizontal tail.

In summary we can say that F4 US Navy flight data base predicted the loads quite well. This leads to the conclusion that the simple engineering loads approach used during the Swiss ASIP study seems to have some draw backs (see figure 7). The flight data was inter- or extrapolated based on a simple AOA dynamic pressure curve which may not take into account the local flow field on all the control surfaces. These results demonstrate the powerful CFD technology for today's loads steady state calculation.

4.2 CFD Calculation on the deformed Wing

The load case C1S825 corresponds to an 8.25 g steady state manoeuvre. At this condition the wing deforms due to the high loads, and one can expect that this change in wing shape will influence the flow over the wing. To investigate this effect an iterative CFD calculation on a flexible F/A-18 wing (with control surfaces) was made. Four iteration steps were needed to reach a converged wing position. During this simulation the fuselage, horizontal stabilizer, vertical tail and rudder were considered as rigid.

The simulation started with the rigid airframe on which the aerodynamic forces are calculated using CFD. These forces are transmitted to the NASTRAN model, which calculates in return the wing deformation. This deformation corresponds to the first iteration, and is applied on the CFD mesh to reshape it around the wing. This procedure was repeated until a converged wing position was obtained.

The deformed wing is shown in figure 8. Note that the missile remains almost parallel to itself; hence we are facing a quite pure bending deformation mode. It can also be seen that the difference in the spatial angle between TEF and aileron was reduced by the deformation of the wing.

The first iteration produced a large deflection. The second and subsequent iterations bring only small corrections, and the third and fourth iterations are almost identical.

The wing bending moment was calculated for all four iterations, and for this quantity the fast convergence was observed as well. A large effect of the wing deformation was observed, since this quantity was reduced with 20% compared to calculation with the non-deformed wing.

5. UNSTEADY STATE CFD AND TRANSIENT CALCULATIONS

5.1 Calculation for C2S825 Load Case

Unsteady calculations were made for the Boeing load case C2S825, which concerns a 8.5 g manoeuvre at Mach=0.7, Altitude 15'000 feet and angle of attack 26.6^o. The dual time stepping approach was used with a constant outer time step of $2.5\ 10^{-4}$ seconds. Two thousand time steps were made, and 0.5 seconds of real time was simulated, see figure 9. The pressure and skin friction vector were saved each outer time step to permit the analysis of the unsteady aerodynamic loads on the aircraft. The calculation ran for about 20 days on a cluster of 6 PC's, and generated 350 GBytes of data. Comparison of the mean unsteady aerodynamic loads with the loads obtained using a steady calculation showed significant differences in loads on the aft fuselage, vertical tail, rudder, trailing edge flap, aileron and horizontal stabilizer, indicating that unsteady flow effects are important on these components of the aircraft.

5.2 Trend Study for Buffeting at the Vertical Tail

The first stub (see figure 10) of the vertical tail attachment to the aft fuselage was elected for this study. From the Swiss full scale fatigue test steady state manoeuvre loads and local strain gauge outputs for the design spectrum were available.

The unsteady flow field generated by the Leading Edge Extension (LEX) vortex produce a time and location dependant pressure field on the vertical tail surface, see figure 11. In order to capture these unsteady forces the fin surface has been divided into 54 (6x9) trapezoidal panels as it is shown in the figure 12. By each time step the resulting force of the pressure acting on both sides of each panel has been calculated using unsteady CFD calculations.

A detailed finite element model of the vertical tail with the six stubs and the flexible attachment to the fuselage originally developed for stress analysis was available by RUAG. 54 lumped masses were included to the model, attached at the central point of each panel and corresponding to the mass of each trapezoidal domain (see figure 13). This dynamic model has been used to calculate the first five ¨Eigenmodes¨ of the vertical tail structure and its rudder. The resulting deformations and frequencies were perfectly satisfactory compared to the measured modes founded in the documentation of the aircraft OEM manufacturer. The frequencies lie between 15 and 85 Hz.

The time dependant aerodynamic panel forces mentioned above have been applied on each node of the lumped masses and a transient calculation of the vertical tail has been achieved for a real duration of 0.5 second and 2000 time steps. This time range is quite short but acceptable with regard to the frequencies, which are interesting for our dynamic investigation.

For this study we focused consequently the evaluation of the fatigue effects taking into account the vertical tail dynamic motion on the connecting elements. We use for this aim the influence coefficient method based on the assumption that the local stress are linearly dependent of the main drivers like the section forces namely the bending moment (BM), the torsion moment (TQ) and eventually the shear force (SH) at the root of the vertical tail (see figure 10). This principle has been also applied by the aircraft manufacturer for stress calculation on different parts of the structure.
To determine the force and the moment vectors at the reference position of the vertical tail root, the pressure and inertia forces have to be added on each of the 54 nodes:

$$\vec{F}(t) = (FX(t), SH(t), FN(t)) = \sum_{1}^{54} (A_i \vec{p}_i(t) - m_i \vec{a}_i(t))$$

$$\vec{M}(t) = (BM(t), PM(t), TQ(t)) = \sum_{1}^{54} \vec{r}_i x (A_i \vec{p}_i(t) - m_i \vec{a}_i(t))$$

FX, SH the shear forces in X und Y direction
FN the normal force in Z direction
BM, PM, TQ bending, pitch and torsion
Ai panel surface
pi panel pressure
mi lumped mass
ai acceleration
(see definitions in figure 10)

The unsteady buffeting forces on the vertical tail create time dependant stresses on the stub with pronounced peaks and valleys. As reported above the BM(t) and TQ(t) could be calculated from the CFD calculation for a duration of 0.5 sec.

Using the influence coefficient formula derived from the full scale fatigue test for the linear combination of bending and torque moment for the manoeuvre loads we get the following peak valley sequence for the corresponding range of time due to buffeting (see figure 14).

It resulted in 26 peaks and an equal number of valleys lying quite symmetrically on both sides of the time axis as expected due to the buffeting loading. By contrast the manoeuvre spectrum is more situated in the tensile domain with an average stress clearly bigger than zero. The extreme values for the buffeting stresses are not so high like for the manoeuvre spectrum. But nevertheless they are considered as having the same order of magnitude.

6. TREND STUDY FOR BUFFETING FATIGUE ANALYSIS

6.1 Buffeting Spectrum Generation

To insert the buffeting sequence in the manoeuvre spectrum a lot of data coming from flight tests are required. The vertical tail buffeting has not yet been enough investigated in flight with Swiss conditions to generate a sufficient data set. From the USN flight tests we know that the buffeting appears essentially by manoeuvre's with angle of attack around 16° and higher, and that the span of time of a real buffeting sequence is heavily dependent on the way how the pilots fly the different manoeuvres.

To overcome this lacking information it has been decided to generate different spectra by varying the limit angle of attack and the buffeting duration of each buffeting sequence in a first simple engineering approach:

Lower Limit for AoA:	18°	19°	20°
Buffeting Sequence (sec)	5	10	20

From the Swiss line by line spectrum the dynamic pressure and the total mass of the aircraft for each manoeuvre are well known but nothing is known about the angle of attack. In order to play back this information an approximated angle of attack calculation has been done using the available manoeuvre data mentioned just above and the aerodynamic lift characteristics of the aircraft.

Using a specific FORTRAN program the buffeting peak valley sequence has been inserted N times after each manoeuvre reaching or exceeding the selected limit angle of attack. Where N is simply calculated by:

N= Buffeting Sequence / 0.5

The Swiss line by line spectrum without buffeting contains 26990 values. After the insertion of the buffeting cycles this number is growing up to 33750 or to 93550 depending on the time interval (5, 10, 20 sec).

6.2 Fatigue Life Calculation

This set of spectrum has been used for the crack initiation life calculation in order to evaluate the effect of the buffeting on the stub at F.S.557.

To produce realistic conditions the following parameters have been chosen for this calculation:

Material: AL7050-T74
Compression Tensile Ratio Kc/Kt 1
Flight Hours Number for LBL Spectrum 200
No Prestain Material Data
Equiv. Strain Equation Smith-Watson-Topper
Reference Stress 17.17 ksi

With the aim to have a comparison with the USN design spectrum an additional case has been calculated using the BM(t) and TQ(t) line by line manoeuvre spectrum of the vertical tail without buffeting. The same influence coefficients are used as calculated above. This line by line spectrum was delivered from the aircraft manufacturer and represents 300 service flight hours.

In the year 1992 different very detailed investigations have been done by the F/A-18 manufacturer in order to quantify the fatigue life due to the buffeting at the vertical tail. One crack initiation life curve of stub F.S.557 with the same metal parameter like indicated above has also been selected in order to have a comparison with the buffeting by the USN conditions.

All theses results were collected in the crack initiation life diagram presented in the figure 15. These crack initiation life curves demonstrate that the simulated buffeting based on CFD unsteady calculation and structural dynamic transient calculation increase the severity of the manoeuvre spectrum in the same order of magnitude like observed in the USN dynamic study.

7. UNSTEADY AERO-ELASTIC COUPLING DEVELOPMENT

To take into account the full structural response due to dynamic aero loads an unsteady aero-elastic simulation tool is required. RUAG started the development of such a tool in early 2005. Essential elements of this tool are:

a CFD solver using the ALE formulation and which includes a re-meshing algorithm to regenerate the CFD volume mesh after the movement of the surface;

a geometrical coupling tool which permits transfer of the aerodynamic loads from the CFD mesh to the CSM mesh, and transfers the structural displacement into the CFD surface geometry displacement;

a CSM solver to compute the structural state. To reduce computational costs a linear structural model is often used, which is further simplified by using a modal formulation. The time integration of the structural equations is made using the Newmark method.

The CFD and CSM solvers are coupled through the geometric coupling tool (the so called segregated or partitioned approach). Within this approach different coupling schemes can be formulated and in a first step the so called Conventional Staggered Scheme (CSS) [1] was implemented. When using the dual time stepping approach for the CFD solver, no coupling between CSM and CFD solver takes place inside the so called inner-loop. This may be sufficient for small deformations of the surface, but for larger deformations a stronger coupling approach may be needed [2].
A new version of the FSI/MI (Fluid Structure Interaction/Modal Integration) library became available in 2006 which permits to couple CFD and CSM in the inner loop of the dual time stepping procedure. Although the computational costs are higher compared to the old implementation, the new implementation permits to use larger outer time steps without the loss of accuracy.
To validate the unsteady aero-elastic simulation tool calculations were made for the AGARD 445.6 wing [3]. The AGARD445.6 wing, made of mahogany, has a 45o quarter chord sweep, a half span of 2.5 ft, a root chord of 1.833 ft and a constant NACA64A004 symmetric profile. Flutter tests were carried out at the NASA Langley Transonic Dynamics Tunnel, were published in 1963 and re-published in 1987. Various wing models were tested (and broken) in air and Freon-12 for Mach numbers between 0.338 and 1.141. The case most often used in the literature is the so called weakened model 3 at zero angle of attack in air. The model was weakened by holes drilled through the surface of the original model to reduce its stiffness.

The linear structural model was build by SMR, with the material properties taken from [4]:

E1	3.15106 106	Pa
E2	4.16218 108	Pa
G	4.39218 108	Pa
ρ	381.98	kg/m3
ν	0.31	

Only the first four mode shapes are considered, consisting of two bending and two torsion modes.

CFD calculations were made for the following free stream conditions

Mach	0.95	
ρ∞	0.061	kg/m3
α	0	
Re	1.196 106	1/m
μ	234.93	

using free stream pressures of respectively 3500, 4600 and 7000 Pa. Experimental data showed that flutter occurs when the value of the flutter speed coefficient (or flutter index) is around Vf = 0.32 ($Vf = U_\infty / (b_s\ \omega_a \sqrt{\mu})$) with U_∞ the free stream velocity, b_s the half span, ω_a the frequency of the first torsional mode and μ the mass ratio. Flutter should occur for the highest free stream pressure, which has a flutter index of 0.383.
The coupled aero-elastic calculations were started from the steady CFD result for the same conditions. Then a 2.5% deflection of the first bending moment was given to the structure and the unsteady simulation was started. A structural damping of 2% was used in the CSM calculation. In the figures 16 and 17 the contour plot of the Mach number is represented for two extreme wing deflections. In the figure 18 one can observe that, conforming to the experimental data and the flutter index in the case 7000 Pa the deflections is growing up, in the two other cases they are damped.

8. CONCLUSION AND OUTLOOK

Component loads for structural and fatigue analysis were calculated using the RUAG inhouse CFD solver NSMB. The calculated loads were in good agreement with the flight loads data.
The interaction of the aerodynamic pressure over wing with the structural stiffness is important and must be considered for the loads calculation using fluid structure interaction. Only within 4 iterations between CFD and CSM a converged solution for the wing was found.
With todays computer performance an unsteady state CFD calculation brings more information into buffeting and flutter behaviour of modern airplanes. With the NSMB unsteady capabilities real flow field for 0.5 seconds over the F/A-18 were processed.
A simple buffeting study for the F/A-18 vertical tail was done to assess the impact of damaging cycles for the fatigue life. The results showed a severity of 5 for the fatigue life compared to the Swiss design manoeuvre spectrum.
To take into account the full structural response due to dynamic aero loads an unsteady aeroelastic interaction tool is necessary. RUAG started this development in early 2005. First an algorithm was established based on the method of Farhat with implicit coupling scheme. The time integration is done with the Newmark algorithm. The tool chain was validated with the AGARD 445.6 wing with experimental data from the literature. This task was completed in 2006. Now RUAG is setting up the first calculation for the F/A-18 vertical tail with full transient aeroelastic coupling. The goal is to establish a design spectrum with buffeting cycles to assess the dynamic impact for the structural integrity for the vertical tail.
The buffeting and flutter should be addressed in an early design phase of a modern airplane. RUAG Aerospace CFD dynamic fluid structure coupling tool may provide an early answer to these problems for the aircraft structural integrity.

REFERENCES

[1] C. Farhat, M. Lesoinne, N. Maman. Mixed explicit/implicit time integration of coupled aeroelastic problems: three-field formulation, geometric conservation and distributed solution. International Journal of Numerical Methods in Fluid, Vol. 21, 1995, no. 10, pp.807-835.

[2] J. Smith, Aeroelastic Functionality in Edge Initial Implementation and Validation, FOI Report R-1485-SE, 2005.

[3] E.C. Yates Jr. AGARD Standard Aero-elastic Configurations for Dynamic Response 1: Wing 445.6 AGARD R-765, 1988, NASA TM-100492, 1987.

[4] G.S. L. Goura, Time marching analysis of flutter using Computational Fluid Dynamics. Ph.D thesis, University of Glasgow, 2001.

Fig. 1: LEX fence F

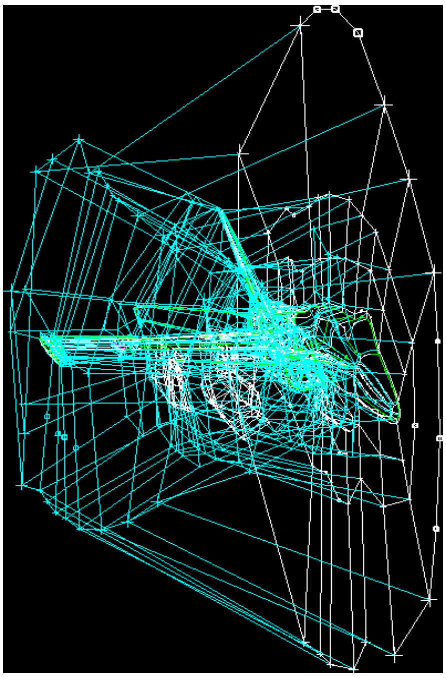

Fig. 2: blocks around the F/A-18

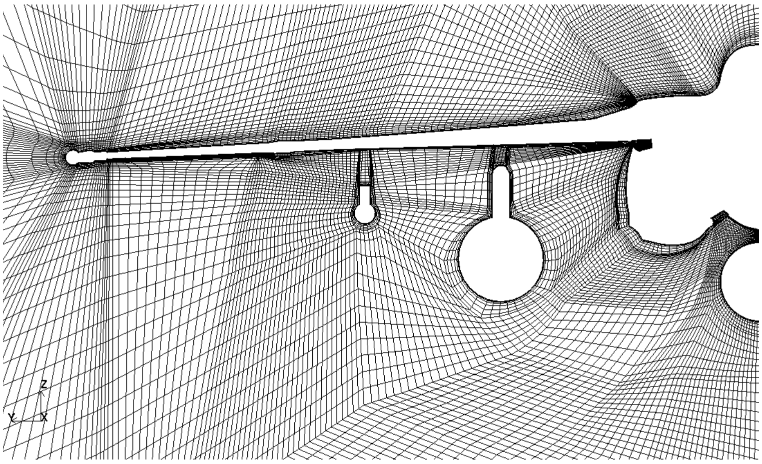

Fig. 3: cut in the mesh of the F/A-18

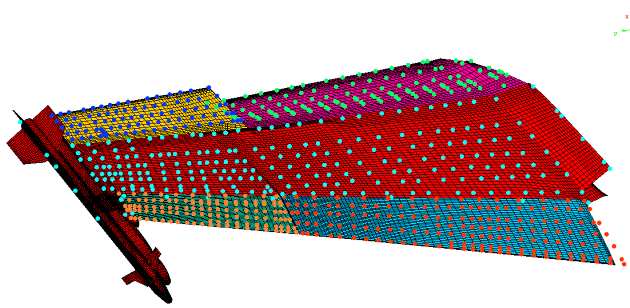

Fig. 4: CFD grid and structure grid (FEM) superimposed

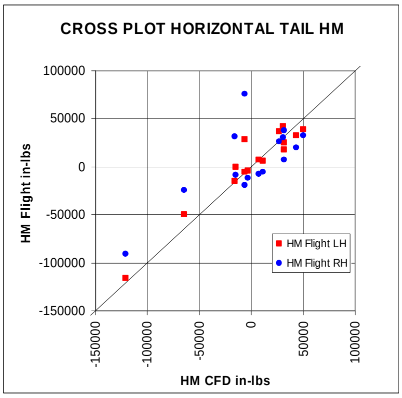

Fig. 5: HT hinge moment crossplot

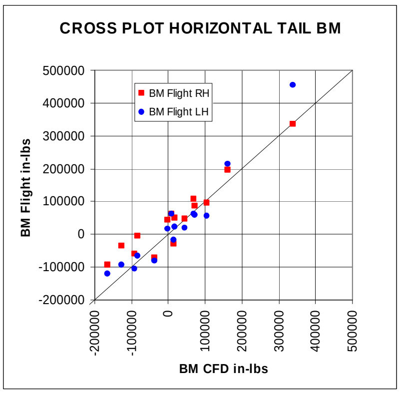

Fig. 6: HT hinge moment crossplot

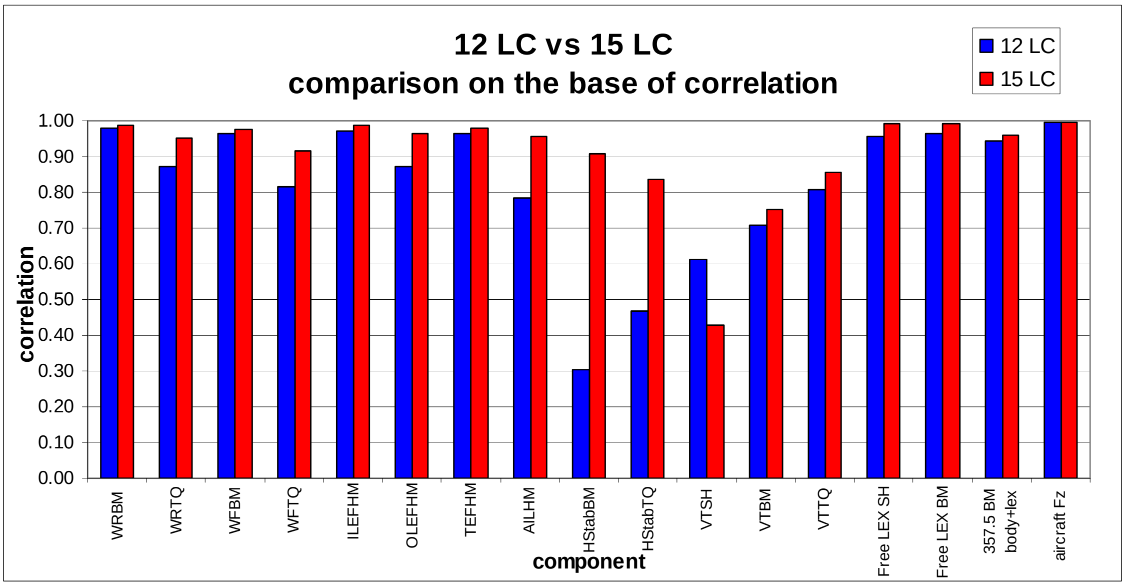

Fig. 7: Correlation grade between OEM-Data and CFD results for component loads
(blue: 12 Swiss ASIP load cases, red: 15 US Navy F4 Flight Load Cases)

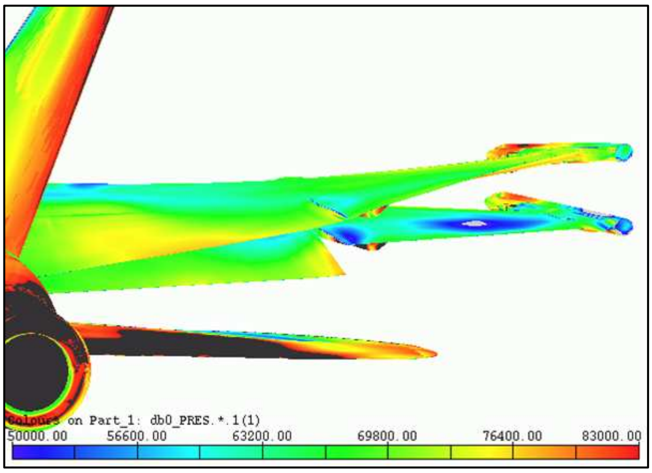

Fig. 8: CFD result of undeformed and deformed wing using fluid structure coupling

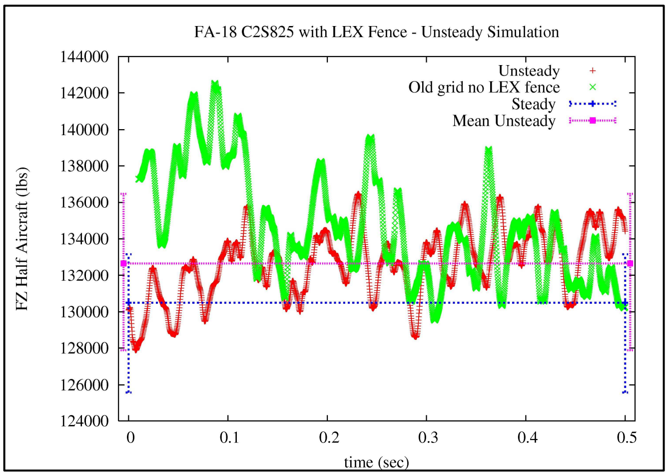

Fig. 9: Lift values for 2000 time steps

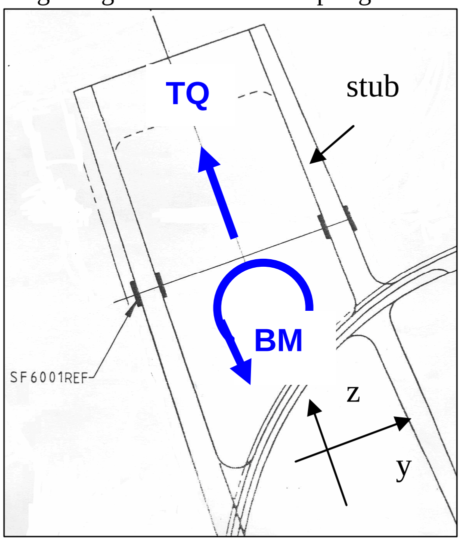

Fig. 10: Definition BM and TQ on the stub

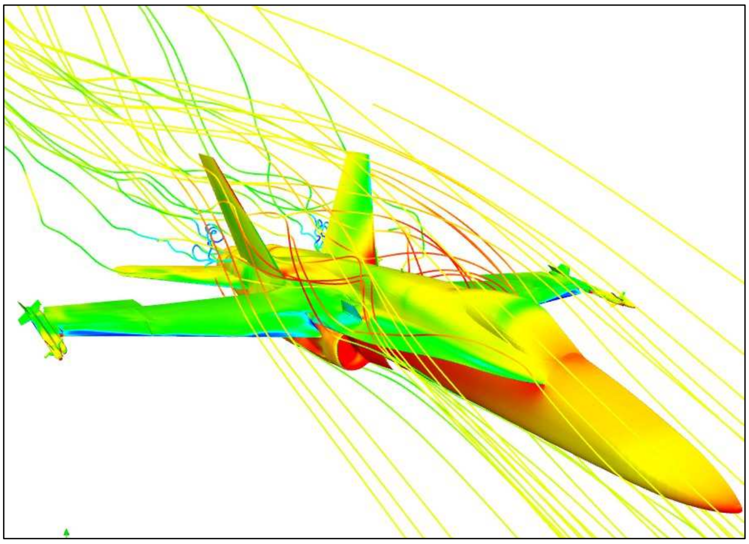

Fig. 11: Influence of unsteadiness at the vertical tail inducing the buffeting

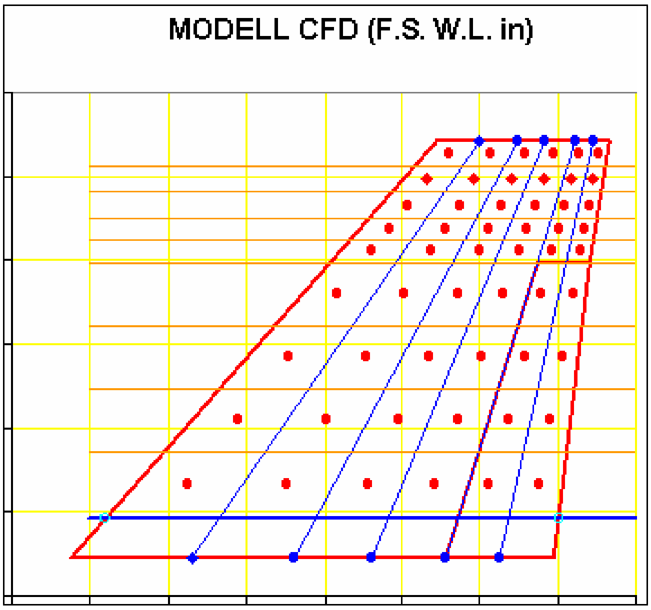

Fig. 12: 54 panels on the vertical tail

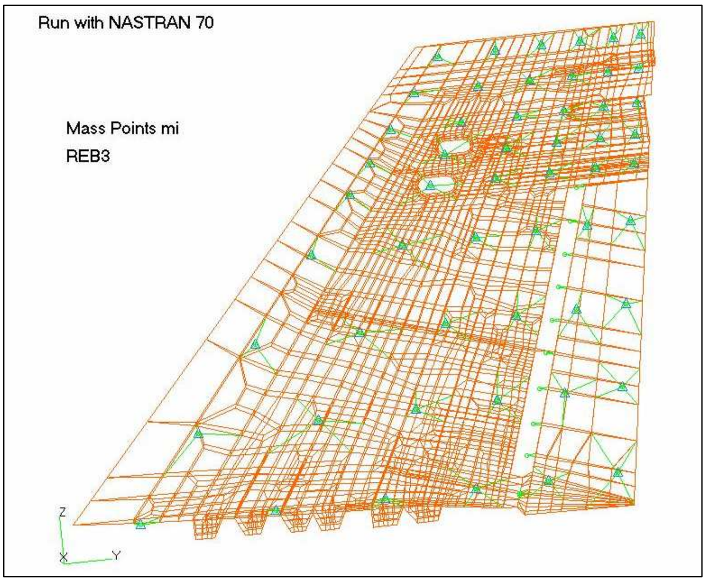

Fig. 13: Finite Element Model with 54 lumped masses

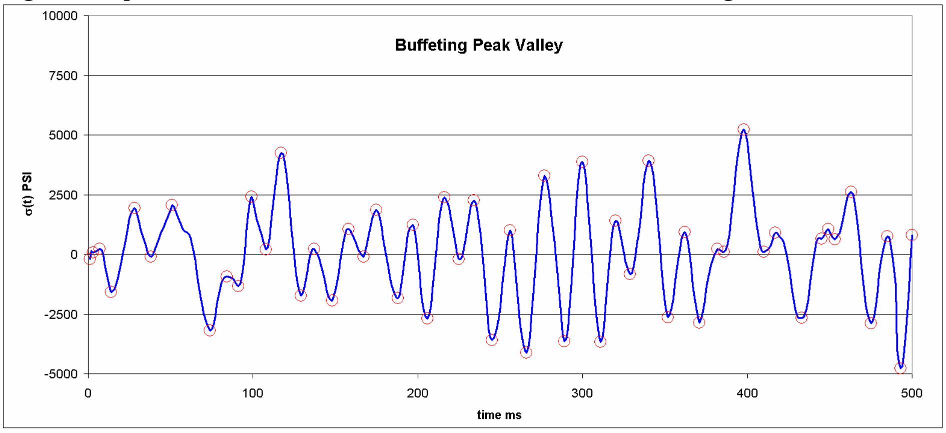

Fig. 14: Peak Valley buffeting sequence

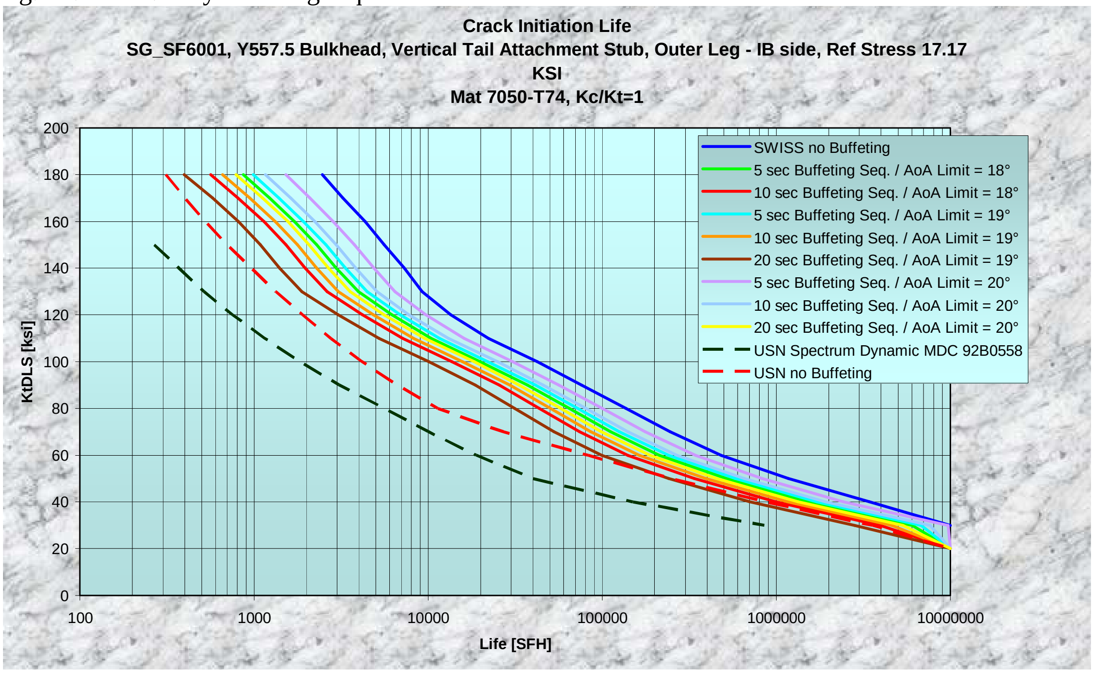

Fig 15: Crack initiation life curves for parameter study and USN spectra

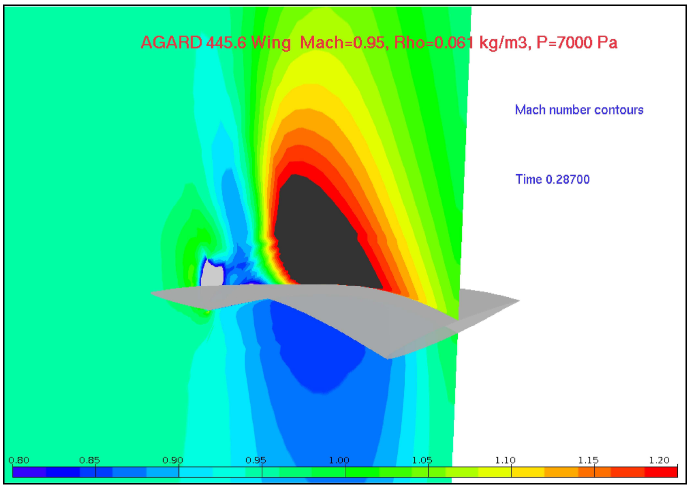

Fig. 14: AGARD 445.6 Wing bending down

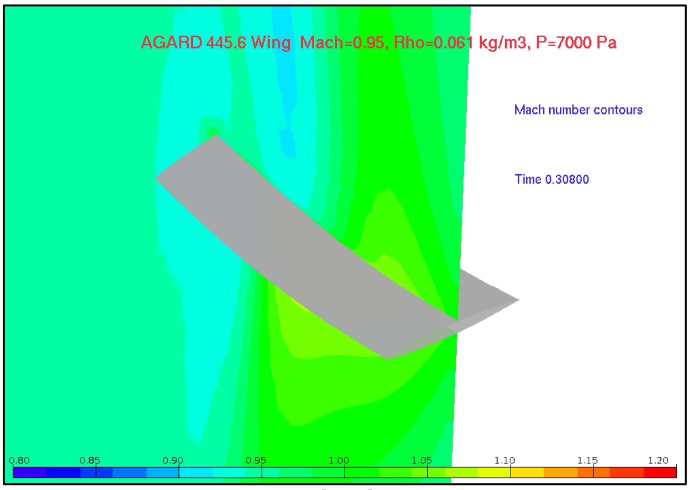

Fig. 15: AGARD 445.6 Wing bending up

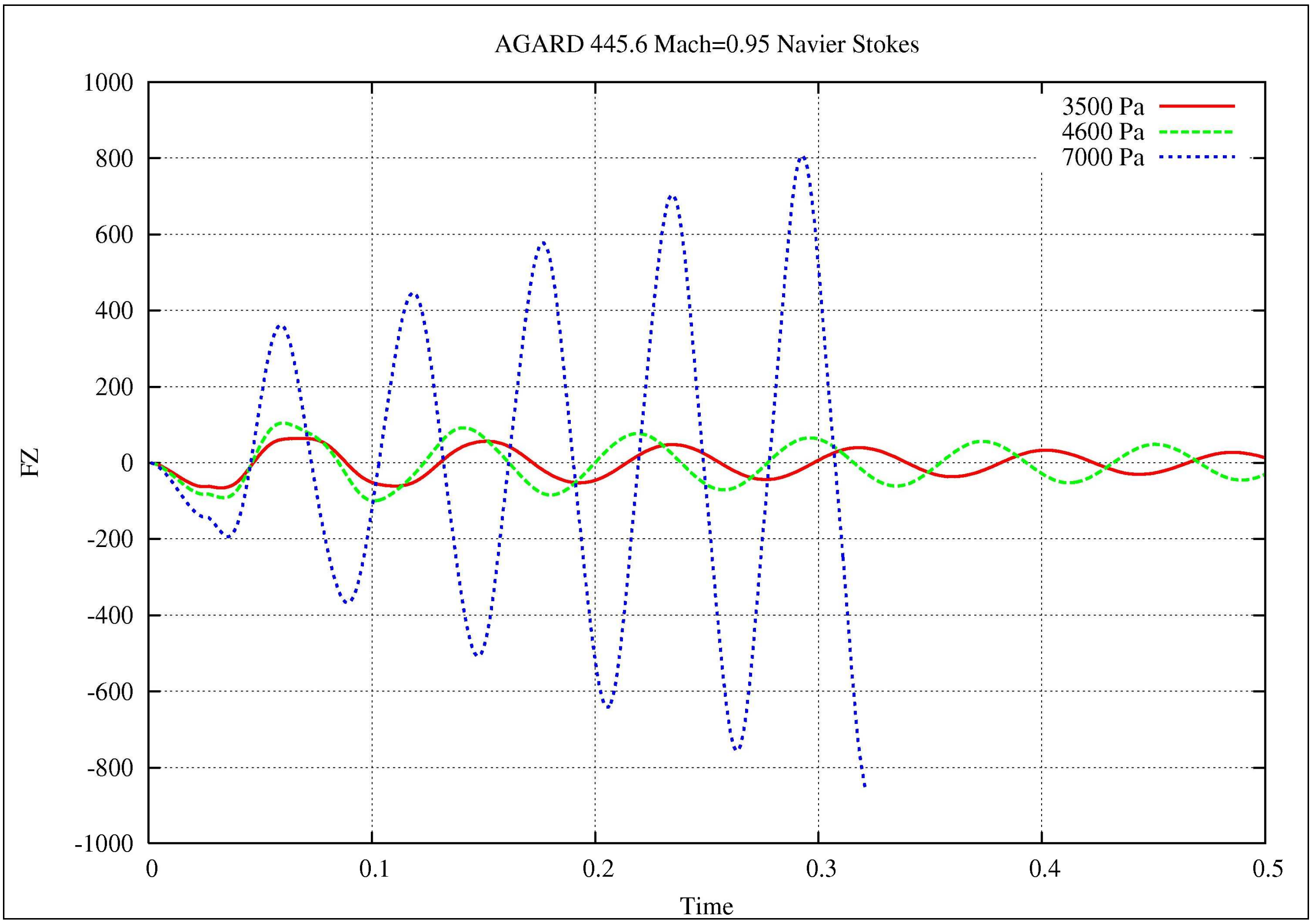

Fig. 16: Time history AGARD 445.6 wing lift force Fz for three cases (3500 Pa, 4600 Pa, 7000 Pa)